# University of Groningen

## Functional MRI for Treatment Evaluation in Patients with Head and Neck Squamous Cell Carcinoma

Nooij, Roland P; Hof, Jan J; van Laar, Peter Jan; van der Hoorn, Anouk

IMPORTANT NOTE: You are advised to consult the publisher's version (publisher's PDF) if you wish to cite from it. Please check the document version below.

*Document Version*
Publisher's PDF, also known as Version of record

*Publication date:*
2018

[Link to publication in University of Groningen/UMCG research database](Link to publication in University of Groningen/UMCG research database)

CrossMark

# Functional MRI for Treatment Evaluation in Patients with Head and Neck Squamous Cell Carcinoma: A Review of the Literature from a Radiologist Perspective

Roland P. Nooij[1] · Jan J. Hof[1] · Peter Jan van Laar[2,3] · Anouk van der Hoorn[2,3]

## Abstract

*Purpose of review* To show the role of functional MRI in patients treated for head and neck squamous cell carcinoma.

*Recent findings* MRI is commonly used for treatment evaluation in patients with head and neck tumors. However, anatomical MRI has its limits in differentiating between post-treatment effects and tumor recurrence. Recent studies showed promising results of functional MRI for response evaluation.

*Summary* This review analyzes possibilities and limitations of functional MRI sequences separately to obtain insight in the post-therapy setting. Diffusion, perfusion and spectroscopy show promise, especially when utilized complimentary to each other. These functional MRI sequences aid in the early detection which might improve survival by increasing effectiveness of salvage therapy. Future multicenter longitudinal prospective studies are needed to provide standardized guidelines for the use of functional MRI in daily clinical practice.

✉ Anouk van der Hoorn
a.van.der.hoorn@umcg.nl

1  Department of Radiology, Medical Spectrum Twente, Enschede, The Netherlands

2  Department of Radiology, University Medical Center Groningen, University of Groningen, Hanzeplein 1, P. O. Box 30.001, 9700 RB Groningen, The Netherlands

3  Medical Imaging Center, University Medical Center Groningen, University of Groningen, Groningen, The Netherlands

**Keywords** MRI · Treatment evaluation · Primary tumor · Lymph nodes · Head/neck squamous cell carcinoma · Review

## Abbreviations

| | |
|---|---|
| ADC | Apparent diffusion coefficient |
| ASL | Arterial spin labeling |
| DCE | Dynamic contrast enhanced |
| DKI | Diffusion kurtosis imaging |
| DSE | Dynamic susceptibility enhanced |
| DWI | Diffusion weighted imaging |
| HNSCC | Head and neck squamous cell carcinoma |
| IVIM | Intravoxel incoherent motion |

## Introduction

Head and neck cancer affects 550,000 new cases and 380,000 deaths worldwide annually [1–3]. Head and neck squamous cell carcinomas comprise over 90% of the head and neck carcinomas [4]. Patients frequently present with a locally advanced stage for which the current therapy is multimodal including surgery, radiation therapy and/or chemotherapy [5–8]. Many patients demonstrate unfavorable treatment response, with locoregional recurrence seen in about 30–60% [7]. This is in about 2/3 due to primary tumor recurrence, 1/3 due to regional nodal metastasis and in 1/3 due to both primary tumor recurrence as well as regional nodal metastasis [9].

Conventional anatomical MRI techniques are commonly used for treatment evaluation, but are often not able to have reliable assess treatment response. Surgery as well as chemoradiotherapy induce false positives on imaging as a

result of inducing benign changes involving architectural distortion, fibrosis and/or necrosis [10••, 11, 12, 13•, 14•]. These benign treatment-induced changes should be differentiated from residual and/or recurrent tumor on imaging to prevent unjustified alteration in treatment plan, e.g. salvage therapy or (dis)continuation of therapy. Early detection of local recurrence could lead to timely salvage therapy which can lead to an increase in overall survival [15–17].

Post-treatment surveillance can consist of ultrasound, PET-CT [18–21] and MRI [10••, 11, 12, 13•, 14•]. Several recent studies have shown the potential usefulness of functional MRI techniques for treatment evaluation in patients with head and neck tumors [10••, 11, 12, 13•, 14•, 22••, 23–28, 29•, 30–33•]. Diffusion-weighted imaging is used to image changes in cytoarchitecture and measure cellular density. Perfusion-weighted MRI techniques can identify tumor-induced neovascularization. Changes in concentrations of metabolites are shown with magnetic resonance spectroscopy (MRS).

This review will analyze the functional MR imaging sequences with regards to their possibilities and limitations in head and neck squamous cell carcinoma. Clinical implications, applicability and possibilities of these sequences for treatment evaluation will be addressed.

## Role of Conventional Anatomical MRI in Head and Neck SCC

Conventional anatomical MRI techniques are used for treatment evaluation. MRI is superior to CT yielding higher anatomical detail [11, 12, 13•, 14•, 34–37]. Anatomical MRI to assess HNSCC should include a T1 without fat suppression, T2 with and without fat suppression and T1 post-contrast with fat suppression. These sequences are used to analyze certain characteristics of the primary tumor and possible nodal involvement [11, 12, 13•, 14•, 34–37].

However, anatomical MRI techniques are often unable to accurately identify treatment response showing a pooled sensitivity and specificity for local treatment response evaluation in HNSCC of 84 and 82%, respectively [22••]. This is due to benign treatment effects such as inflammation, fibrosis and necrosis as a result of surgery and chemoradiotherapy. These post-therapy changes show overlapping signal characteristics with tumor. Most problematic for the primary site is that inflammation and tumor both show high T2 signal and enhancement after contrast injection. Lymph node assessment is most hindered by reactive lymph node that can be slightly enlarged similar to nodal metastasis. Furthermore, normal sized nodes can still contain tumor. See Table 1 for a detailed description of the signal intensities on anatomical MRI post-treatment.

Higher diagnostic accuracy than 84% sensitivity and 82% specificity post-therapeutically is needed to differentiate treatment effects from true malignancy for the local tumor site and the regional lymph nodes to reliable either initiate new therapy, adjust the current therapy or discontinue unjustified therapy.

## Technical Background of Functional MRI Techniques

### Diffusion Weighted Imaging

DWI measures cellular density and cytoarchitecture using the measurement of water diffusivity. Random diffusion results from the Brownian motion of water molecules. Motion of water molecules is hindered, restricted, by interactions with other molecules and cellular barriers such as fibers, cell membranes and macromolecules. Diffusion abnormalities of water molecules thus reflect changes of tissue organization at a cellular level affecting the MR signal of a DWI sequence as can be seen in a number of processes including malignancy [10••, 11, 12, 13•, 14, 22••, 24••, 25••, 26–28, 29•, 30, 32, 33•].

DWI sequences are based on a T2-weighted sequence. At least two $b$ values are needed to analyze motion of water. DWI is done at different $b$ values (in s/mm$^2$), which represent the duration between the gradient pulses used. Simplified, it is the time that water is allowed to diffuse before the distance is measured. Most commonly, a $b0$ and $b800$ or $b1000$ value are used for head and neck imaging. Diffusion is quantified using ADC in mm$^2$/s. Having measured at least two different $b$ values (e.g. $b0$ and $b800$), the logarithm of relative signal intensity of a tissue is plotted on the $y$ axis against the $b$ values on the $x$ axis. The slope of the line fitted through the plots describes the ADC. This mono-exponential fitting represents a rough approximation of ADC and is most often used in clinical routine. This parameter is independent of the magnetic field strength. Lower values indicate more restricted diffusion. However, mono-exponential fitted ADC values cannot separate the pure molecular diffusion from the motion of water molecules in the capillary network [32]. Low $b$ values are most influenced by the capillary component which influences the ADC values. Multi-exponential models using several $b$ values are more suitable for accurate quantification of diffusion without perfusion contamination [30, 32, 33•].

Acquiring multiple $b$ values yields techniques such as intravoxel incoherent motion (IVIM) and diffusion kurtosis imaging (DKI). IVIM imaging can distinguish between pure molecular diffusion and motion of water molecules in the capillary network through a single DWI acquisition

**Table 1** Use of conventional anatomical MRI for treatment evaluation

| Anatomical MRI sequence | Primary tumor | Lymph nodes |
|---|---|---|
| T1 without fat suppression | Anatomical details | Anatomical localization of node levels |
| | Tumor: ↓ compared to fat | Metastatic lymph nodes: Size ↑/↑↑ (suggested cut-off > 7–10 mm for level II and > 5–7 mm for all other levels). Round shape |
| | Fat infiltration by tumor or inflammation: similar ↓/↓↓ | Reactive lymph nodes: Size =/↑ (can be false-positive using above cut-off); Oval with fatty hilum |
| | Necrosis: ↓↓ round, oval, well circumscribed | Location of lymph node and level in relation to location primary tumor |
| | Fibrosis: Linear commonly ↓↓, but can be ↓/= as well | |
| T2 with and without fat suppression | Fat suppression useful for the detection of abnormalities | Fat suppression needed to identify abnormal nodes |
| | T2 without fat suppression for anatomical details | T2 without fat suppression for anatomical details |
| | Edema, fat infiltration by tumor or inflammation: similar ↑/↑↑ | Metastatic lymph nodes: ↑ slightly heterogeneous; more commonly an irregular border; possible extra-nodal extension |
| | Necrosis: ↑↑ round, oval, well circumscribed | Reactive lymph nodes: = |
| | Perineural spread: ↑ | |
| | Fibrosis: Linear commonly ↓↓, but can be ↓/= as well. | |
| T1 post-contrast with fat suppression | Fat infiltration by tumor or inflammation: similar ↑/↑↑ | Fat suppression needed to identify abnormal lymph nodes |
| | Edema or necrosis: no enhancement | Metastatic lymph nodes: ↑/↑↑, thick, irregular rim enhancement in case of necrosis |
| | Fibrosis: no enhancement after 6-12 months. Most commonly ↑/↑↑ | Reactive lymph nodes: =/↑ |
| | Perineural spread: ↑↑ | |

High signal intensity is indicated as ↑, low signal intensity is indicated as ↓ and intermediate signal as =

technique if both low $b$ values ($< 200$ s/mm$^2$) and high $b$ values ($> 200$ s/mm$^2$) are used. The relationship between signal intensities and multiple $b$ values can be assessed. Real diffusion of water molecules (D) can be distinguished from the contribution of perfusion to the signal decay (D*) and the contribution of perfusion to the diffusion signal (f). Another, multiple $b$ value method, DKI, represents the extent to which the diffusion pattern of the water molecules deviates from a perfect Gaussian curve that is assumed calculating standard ADC values. Table 2 includes the most commonly used parameters for the different diffusion techniques.

## MR Perfusion

Perfusion is defined as the steady-state delivery of blood to tissue. Several perfusion techniques are available; dynamic contrast-enhanced (DCE) perfusion, dynamic susceptibility contrast (DSC) perfusion and arterial spin labeling (ASL) all yielding different parameters (see Table 2).

DCE perfusion is most commonly used for the head and neck area. DCE is based on the T1 relaxivity effects of contrast agents. DCE perfusion has been reported as a technique which is able to characterize perfusion and vascularization of tissues [24••, 25••, 30–33•]. However, this has not always been histologically confirmed [25••, 38, 39]. Ktrans is the most commonly derived quantitative parameters representing capillary permeability and seems to be to most consistent parameter [24••, 25••, 40].

DSC perfusion exploits the susceptibility-induced signal loss after administration of contrast on T2-weighted sequences, most commonly a quick T2* gradient echo sequence. It is based on inhomogeneity of the magnetic field during the passage of a short bolus of contrast through a capillary bed [27]. As result on the T2* sequence, blood products, calcifications and aerated structures result in artificial signal loss. Mean transit time, blood flow and blood volume can be calculated. However, in the head and neck area a multitude of artifacts are present (e.g. voluntary/involuntary motion, breathing, air-to-tissue surface artifacts) [10••, 11, 12, 13•, 14•], affecting the reliability of the results acquired with DSC.

ASL is a perfusion technique without injection of contrast. Arterial blood is magnetized below the volume of

**Table 2** Use of functional MRI for treatment evaluation

| Functional MRI sequence | Most used parameters | During treatment primary tumor and lymph nodes | After treatment primary tumor | After treatment lymph nodes |
|---|---|---|---|---|
| Diffusion | DWI: ADC, ADC-ratio (= $ADC_{2000}/ADC_{1000}$ × 100%)<br><br>IVIM: D, D*, $f$<br><br>DKI: skewness of distribution | Locoregional control: %ADC ↑ tumor and lymph nodes<br><br>Locoregional failure: %ADC ↓ tumor and lymph nodes. Cut-off range 14–24% [32, 55, 65] | Tumor:<br>ADC↓↓ and $b$800–1000 ↑↑<br>Peritumoral inflammation:<br>ADC ↓/= and $b$800–1000 =/↑<br>Necrosis/apoptosis:<br>ADC ↑/↑↑ and $b$800–1000 ↑/↑↑<br>Edema:<br>ADC =/↑ and $b$800–1000 =/↑<br>Fibrosis:<br>ADC = and $b$800–1000 =<br>IVIM/DKI: ? | Metastatic lymph nodes:<br>ADC ↓↓ and $b$800–1000 ↑↑. Suggested ADC cut-off $1.1 \times 10^{-3}$ $mm^2$/s<br>Reactive lymph nodes:<br>ADC ↓/= and $b$800–1000 =/↑<br>IVIM-derived D and f contradicting literature [35, 38]<br>DKI: ? |
| Perfusion | DCE: AUC, Ktrans, rate constant, extravascular volume and plasma space volume or flow<br><br>DSC: blood volume, blood flow, mean transit time, wash out<br><br>ASL: blood flow | Local control:<br>Ktrans =/↑ [42].<br>AUC =/↑ [42].<br>Plasma flow =/↑ [66].<br>Local failure:<br>Ktrans ↓/= [42]<br>AUC ↓/= [42]<br>Plasma flow ↓/= [66]<br>Regional control (lymph nodes): ? | Tumor:<br>Ktrans ↑, blood volume ↑, blood flow ↑, wash out ↑<br>Peritumoral inflammation: =/↑<br>Necrosis/apoptosis: all ↓<br>Edema: ↓/=/↑ ?<br>Fibrosis: all ↓ | Metastatic lymph nodes:<br>blood flow ↑, blood volume ↑, Ktrans ?<br>Reactive lymph nodes:<br>blood flow =/↑, blood volume =/↑, Ktrans ? |
| Spectroscopy | Concentration of lactate (1.3 ppm), N-acetyl-aspartate (2.0 ppm), creatine (3.0 ppm) and choline (3.2 ppm). Ratios can be calculated | Increased choline, decreased creatine and increase choline/creatine ratio in primary tumor recurrence and nodal metastasis is suggested, although insufficient data available to reliably provide insight [62–64] | | |

See technique section of the paper for explanation of the most commonly used parameters. Suggested cut-off values are given if available. High values are indicated as ↑, low values are indicated as ↓ and intermediate values are indicated as = . References are given if relevant with numbers corresponding to the reference listed in the text

*ADC* apparent diffusion coefficient, *ASL* arterial spin labeling, *AUC* area under the curve, *IVIM* intravoxel incoherent motion, *D* diffusion of water molecules, *D\** perfusion contribution to the signal decay, *DCE* dynamic contrast enhanced, *DKI* diffusion kurtosis imaging, *DSC* dynamic susceptibility enhanced, *f* contribution of perfusion to the diffusion signal, *Ktrans* capillary permeability, *ppm* parts per million

interest. After a certain period, the magnetized blood flows into the volume of interest and its derived signal is measured. Blood flow can be calculated, which could reflect neovascularity and angiogenic activity of malignancy [32]. ASL also uses T1 relaxation, but is challenging as timing of the signal read-out should be precise. Acquiring the volume of interest too late, and the magnetized arterial blood has already passed. However, ASL is feasible in

head and neck cancer using an Locker–Locker sequence [41] or a pseudo-continuous sequence [42].

## MR Spectroscopy

MRS is a technique that detects the presence of specific metabolites. Different metabolites have small differences in their intrinsic vibration frequency and thereby result in small differences in signal of $^1$H protons. Spectroscopy is

thus well-suited to detect changes in the components of tissue due to tumor after suppression of the abundant water signal [43]. Single voxel and multivoxel techniques are able to characterize tissue including the measurements of lactate, *N*-acetylaspartate, creatine and choline. Spectroscopy should be regarded as complimentary to the already acknowledged functional MRI techniques in assessing HNSCC.

## Response Evaluation During Therapy

### Diffusion Weighted Imaging

A rise in ADC is seen after the treatment in HNSCC (Fig. 1) and can be seen already in the first few weeks [24••, 29•]. This percentage increase in ADC has been shown to be a predictor of treatment response [24••]. A smaller mean ADC in the first 3 weeks after treatment start was shown in patients with disease failure compared to those with disease control [29•, 33•, 44]. Three other studies found thresholds of < 14–24% to be predictive for regional failure in using clinical outcome data with at least 2 years follow-up [26, 45, 46]. However, it must be noted that imaging is generally not performed within the first couple of weeks in standard clinical practice.

It is of great importance to interpret ADC analysis in conjunction with anatomical imaging. Areas of necrosis may take longer to resolve than solid areas. In the interim, the necrosis may become organized and show a fall in ADC value [24••]. Therefore, it is critical to identify sites of necrosis that need to be excluded from ADC analysis [24••]. Furthermore, the development of mature scar tissue may also decrease the ADC value [27]. The same holds for compact fibrosis which can demonstrate lowered ADC values and low to intermediate T2 signal.

### MR Perfusion

Vascular HNSCCs are thought to have better treatment response compared to less vascular HNSCCs because of better delivery of chemotherapeutic agents and greater radiosensitivity [24••]. On the other hand, vascular tumors may have a poorer outcome because they are thought they have greater metastatic potential [24••]. Reports suggest that a fall in blood volume is associated with poor overall survival. On the other hand, an increased area under the curve is associated with local control [39]. The early rise in volume transfer (Ktrans) is speculated to result from damaged blood vessels causing them to temporarily become leakier, which potentially could increase the delivery of chemotherapeutic agents into the tumor.

Also plasma flow has shown to react in patients undergoing induction chemotherapy for the regional tumor [47]. The median baseline tumor plasma flow was 53 ml/100 ml/min in 25 responders and 24 ml/100 ml/min in 12 non-responders. In lymph nodes, differences were not significantly different between non-responders and responders [47]. After appropriate validation, this method may be potentially used to guide treatment modification in patients.

### MR Spectroscopy

To the best of our knowledge, only one in vitro study of tumor specimens by has shown significantly elevated pre-treatment choline-to-creatine ratios in a poor response group, but these findings could not be confirmed in an in vivo human study using choline/creatine ratios as well choline/water ratios [48].

## Imaging Primary Tumor Site Post-therapy

### Diffusion Weighted Imaging

Anatomical MRI is mandatory for an accurate delineation of anatomical details (see Table 1). However, anatomical MRI is hindered by interpretation difficulties in the detection of local primary tumor recurrence [10••, 11, 12, 13•, 14•]. A diffusion-derived $b$ 800 or $b$1000 map provides high lesion-to-background contrast, outperforming conventional T2-weighted sequences in this aspect. The accompanying ADC indicates whether the high signal on the $b$ value map is indeed due to tumor recurrence if low signal is seen on the ADC map. If the high signal on the $b$ value map is accompanied by high signal on the ADC map it is not due to tumor and represents T2-shine-through, or increased diffusivity (see also Table 2 for interpretation of functional MRI). Fibrosis also lacks diffusion restriction (Fig. 2). A large meta-analysis showed a higher diagnostic accuracy for ADC compared to anatomical MRI. Anatomical MRI yielded a pooled sensitivity and specificity of 84 and 82%, respectively. ADC showed a pooled sensitivity and specificity of 89 and 86%, respectively [22••]. More recent studies demonstrate a similar diagnostic accuracy for ADC values [46]. Even higher $b$ values up to $b$2000 do not increase the diagnostic accuracy [44, 49]. Using both a $b$1000 and $b$2000 and ADC$_{ratio}$ (= ADC$_{2000}$/ADC$_{1000}$ × 100%) can be calculated. The ADC$_{ratio}$ might increase the diagnostic accuracy although results are variable with a sensitivity and specificity of 63 and 84%, respectively, for one study [44]. This is a small study with 32 patients, thus should be further studied in a large population.
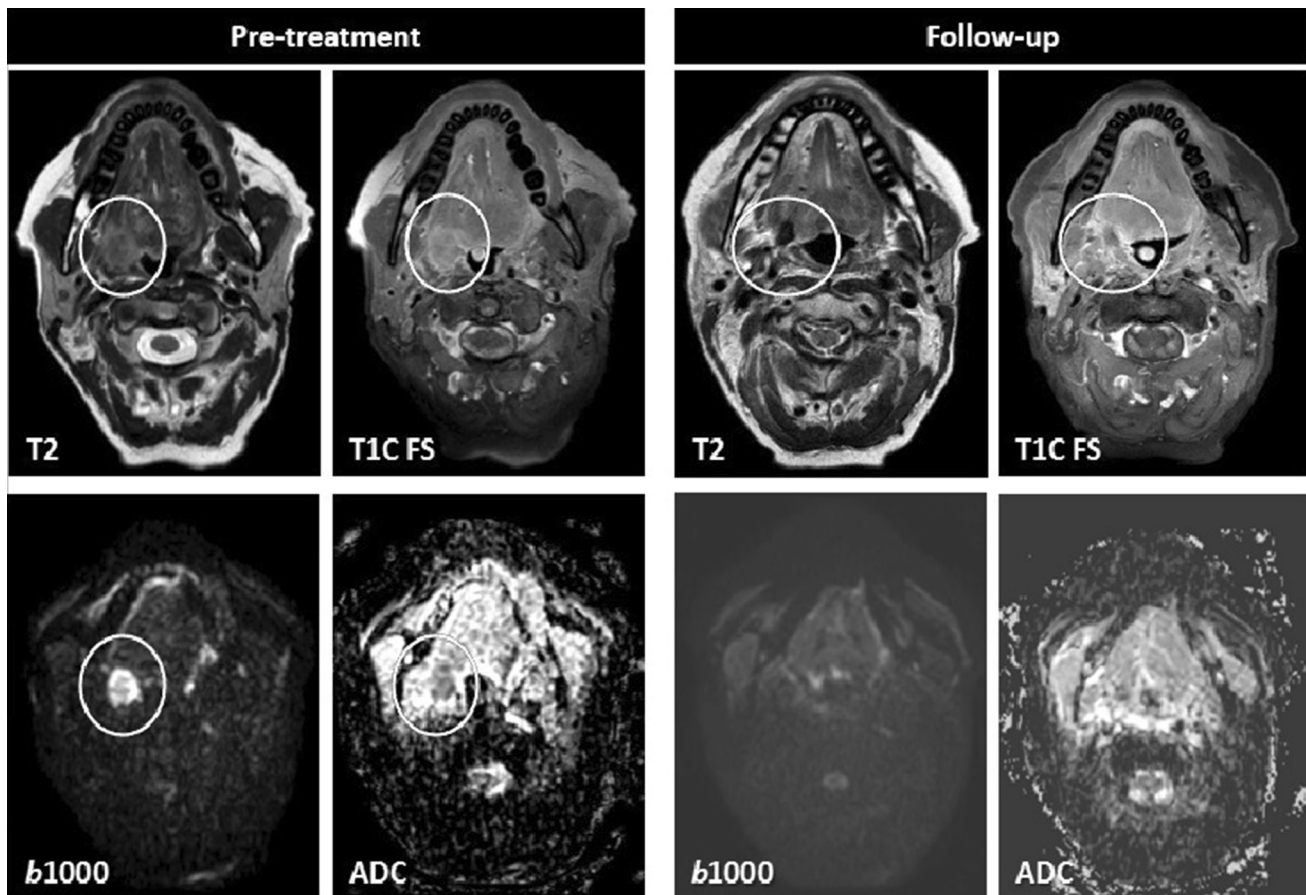
**Fig. 1** Tumor response confirmed on diffusion. A 54-year-old patient with a tumor at the retromolar trigonum showing high T2 signal, enhancement and diffusion restriction before treatment. Follow-up 6 months after radiation therapy showed at least partial response on anatomical MRI with some residual high T2 signal and enhancement. Diffusion restriction aided in the differentiation between residual tumor and post-therapy inflammation. Lack of diffusion restriction in this patient was in keeping with post-therapy changes

Diffusion restriction results from high cellularity as in tumor, but can be also induced due to inflammation and abscesses. Moreover, restricted diffusivity can be seen in normal structures (e.g. Waldeyer's ring or normal lymph nodes) because these structures have an inherent high cellularity [10••, 11, 12, 13•, 14•]. Apoptosis and tumor necrosis can lead to decreased cellularity resulting in an increased diffusivity [24••, 25••, 29•]. This should be kept in mind when interpreting DWI.

## MR Perfusion

A cross-sectional study demonstrated significant differences between DCE perfusion parameters comparing the blood volume of scar tissue and tumor recurrence in HNSCC [50]. Its potential use in treatment follow-up was also shown in a small retrospective study [51]. Although DSC is not the most used perfusion method in the head and neck area, a higher wash-in on DSC has been related with tumor recurrence instead of treatment changes in a prospective study [33•]. However, diagnostic accuracy studies to differentiate treatment changes from tumor recurrence or residual with DCE or DSC perfusion are lacking. Although, visual assessment is possible (see also Table 2 for interpretation of functional MRI), further quantification is currently hindered by standardization of scan parameters and thresholds. In our experience, the area under the curve (AUC) summing the enhancement in a certain voxel, delineates abnormalities most easily with high values for tumor. Relative enhancement provides more insight in the magnitude of enhancement compared with the pre-contrast values. Region of interest analyses could demonstrate relative enhancements curves with the internal carotid artery as reference. A rapid wash-in comparable with the carotid artery followed by a wash out or plateau phase is indicative of tumor (Fig. 3), while slowly progressive enhancements indicate benign treatment changes (Fig. 4).
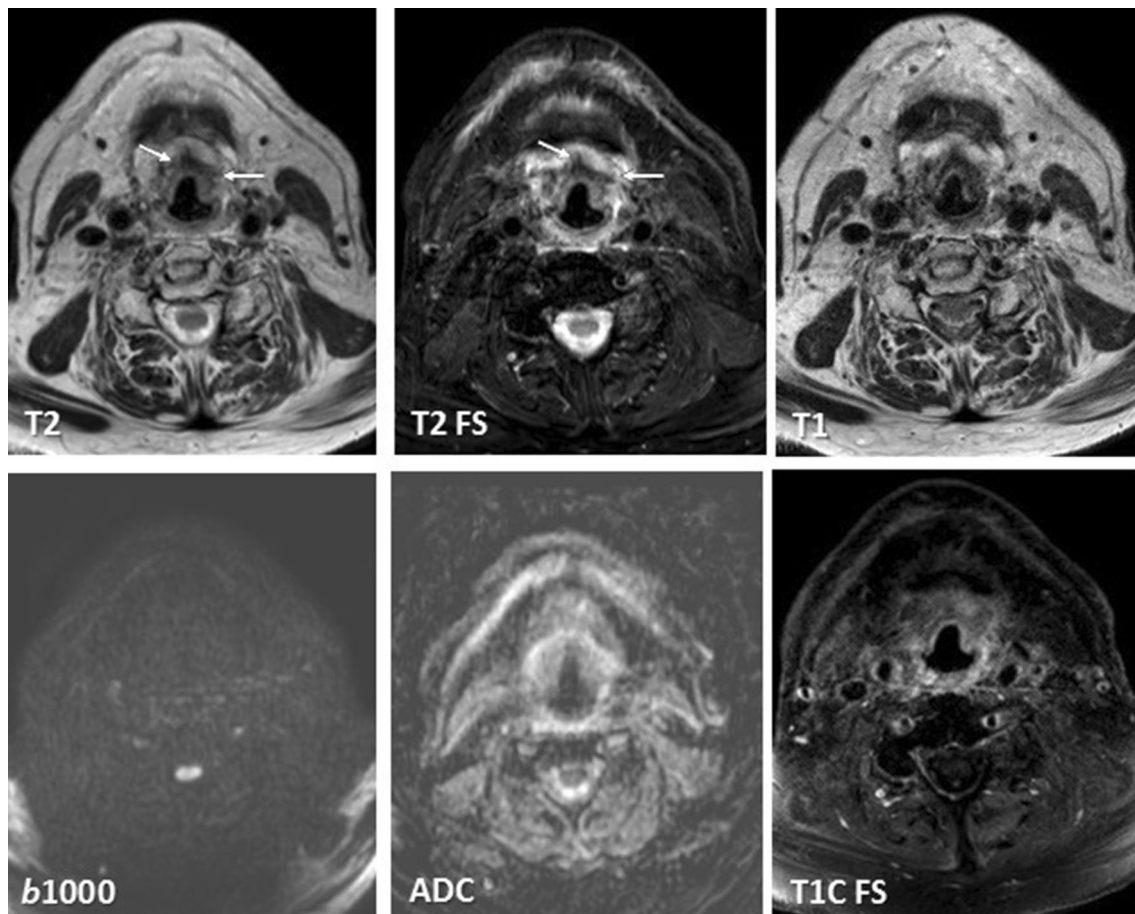
**Fig. 2** Fibrosis on follow-up MRI confirmed with diffusion. A 67-year-old patient with a T3 vallecula tumor showed fibrosis after radiation therapy with low signal on T1 and T2, no enhancement and no diffusion restriction

## MR Spectroscopy

MRS is not routinely used for the treatment evaluation of HNSCC. However, the presence of choline as indication of proliferation and cell membrane turnover yield high specificity of 100%, although false-negative are frequently present, resulting in a very low sensitivity of 44% [52].

## Imaging Lymph Nodes Post-therapy

### Diffusion Weighted Imaging

Treatment evaluation of regional lymph node is less studied than the primary tumor site. A higher diagnostic accuracy for ADC over anatomical MRI is suggested [22••, 53–55]. Anatomical MRI sensitivity and specificity ranged between 67–90 and 33–97%, respectively [22••]. For ADC, this was 78 and 88% in one study and 73 and 100% in another study [45, 53]. However, the difference was statistically not significant. Benign lymph nodes demonstrate higher ADC values compared to malignant lymph nodes

[54–56]. This is also demonstrated in lymph nodes between 5 and 10 mm [54–56]. However, mean ADC values for benign lymph nodes range from to 1.1 to $1.6 \times 10^{-3}$ mm$^2$/s, while HNSCC metastatic nodes range between to 0.78 and $1.1 \times 10^{-3}$ mm$^2$/s [24••, 25••]. A threshold of 1.1, therefore, seems most appropriate to use, although overlap could result in false-positive and false-negative results. The diagnostic accuracy for post-treatment lymph nodes using the IVIM or DKI methods might be better using multiple $b$ values. This remains speculative currently as diagnostic accuracy studies are lacking post-therapy. The values of the known decrease of kurtosis of lymph nodes during treatment [57, 58] should be further established. The IVIM-derived D values represent pure diffusion without perfusion components. Significantly higher D values are demonstrated in patients with regional failure in line with the ADC results [29•, 33•]. However, another study showed no significant rise in $D$ values but a higher initial $f$ value (perfusion fraction) in locoregional failure compared to locoregional control [53].
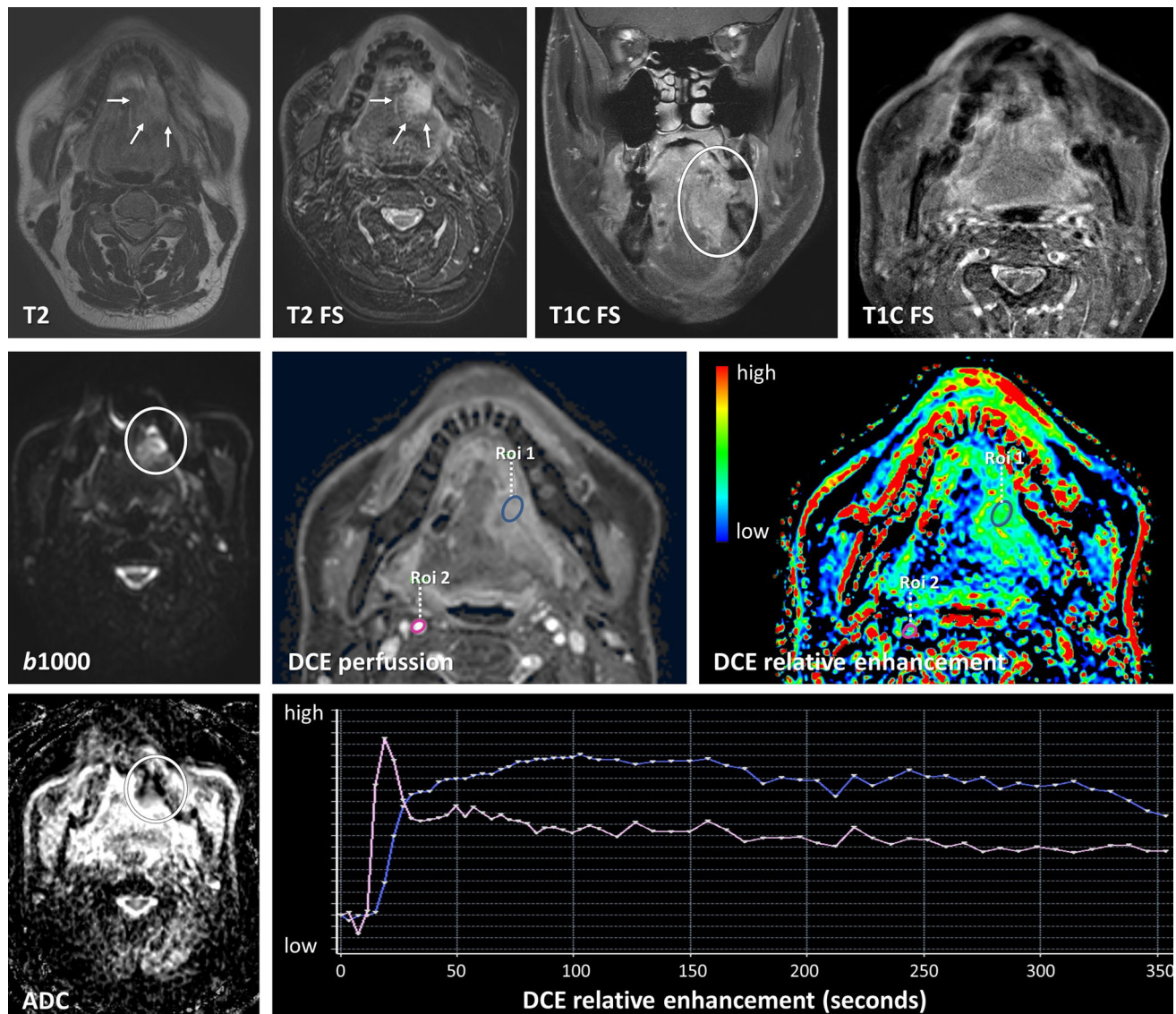
Fig. 3 Tumor recurrence differentiated using diffusion and perfusion. A 57-year-old patient with a total resection of a pT2N0Mx lateral tongue carcinoma. Because of small free resection margins, a second resection was performed 1 month later with a submandibulectomy and free radial forearm flap reconstruction. Anatomical MRI showed changes during follow-up 6 months after resection with high signal on T2 with and without fat suppression. There is enhancement post gadolinium. Anatomical MRI was difficult to interpret as these findings could be due to both tumor recurrence as well as inflammation. Functional MRI demonstrated findings in keeping with tumor recurrence. Diffusion restriction was shown with high $b1000$ and low ADC values. Perfusion demonstrated increased AUC. Relative enhancement of the tumor (blue) showed a wash-in comparable to the carotid artery (purple) with plateau phase indicative for tumor. Tumor recurrence was pathologically confirmed (Color figure online)

## Perfusion-Weighted Imaging

A few recent studies have demonstrated differences in perfusion parameters between benign lymph nodes and malignant lymph nodes [24••, 33•, 41, 42]. Perfusion of nodal metastasis might be increased (Fig. 5). Metastatic lymph nodes demonstrate higher blood flow and blood volume compared to benign lymph nodes on CT perfusion [41, 42], which thus would be expected to be similar for DSC MRI perfusion. The capillary permeability (Ktrans) correlates with the hypoxia-induced transcription factor in the tissue, which is known to stimulate angiogenesis [59]. However, interpretation of MR perfusion in post-therapy lymph nodes is difficult and it remains to be elucidated whether differentiation of malignant and benign lymph nodes can be done reliable (Fig. 6).
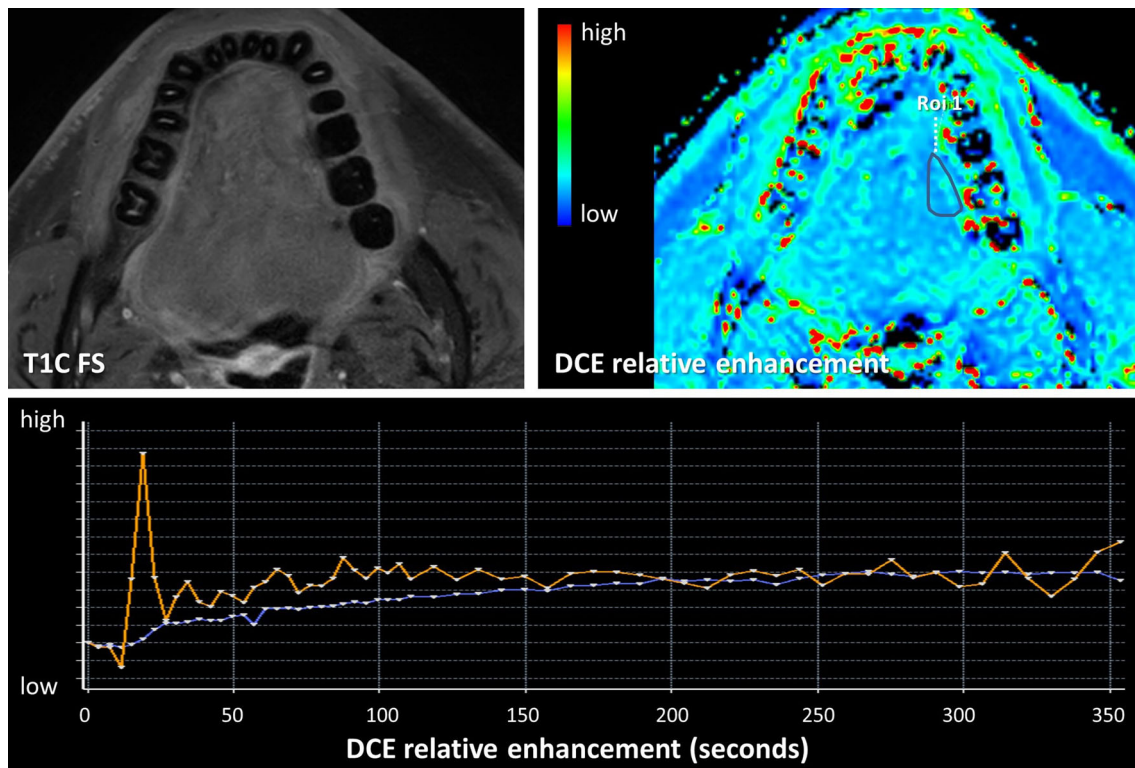
**Fig. 4** Benign perfusion profile post-therapy. A 45-year-old patient with a T1 tongue carcinoma after resection. The primary site showed some enhancement after gadolinium injection on the T1 with fat suppression. A benign perfusion profile is seen with slowly progressive relative enhancement (Color figure online)

## MR Spectroscopy

Acquiring MRS in lymph nodes is currently not clinically applicable as the region of interest should be placed separately on each suspicious lymph node by a radiologist on site. If the technically challenges are overcome, the increased choline, decreased creatine and subsequently increased choline/creatine ratio of metastatic nodes need to be confirmed in larger studies [60–62].

## Limitations

The limitations and potential pitfalls of the functional MRI sequences should be kept in mind during the interpretation. First, the lack of anatomical information at high $b$ values in DWI is a drawback because of suppressed signal in most of the normal tissues. Therefore, DWI should not be interpreted alone, but in correlation with anatomical sequences. This is also true for perfusion and spectroscopy which means that all functional MRI sequences can never be used without the use of anatomical sequences. Moreover, all functional sequences are currently hindered by high variability of cut-offs and parameters used.

Second, it must be stressed that functional MRI remains technically challenging to perform due to artifacts (i.e. breathing, swallowing, involuntary motion and air-tissue interfaces) [10••, 11, 12, 13•, 14•, 24••, 25••, 29•, 32, 33•]. Moreover, acquisition parameters have yet to be standardized. Examples of protocols for the functional MRI sequences of the head and neck are described and could be used as a guide when implementing these sequences [24••].

Diffusion-derived interpretation is mainly done using mean ADC values. Diffusion showed good reproducibility for baseline scans for the ADC value of the primary tumor and nodal metastasis [63]. The reproducibility of the ADC during treatment is also suggested to be good [64]. Mean values of the tumor or metastatic lymph node are not representative when they consist of both highly and poorly cellular (necrotic) portions. Mean ADC values should be measured in the areas with high cellularity only to overcome this limitation [24••, 25••]. Even then, ADC interpretation remains challenging. A recent study suggested a reduced field of view (FOV) might increase accuracy [65]. Moreover, it has been suggested that multiple $b$ values are more accurate as this method is able to distinguish the perfusion component resulting in a pure diffusion value. This perfusion might influence the ADC value, although
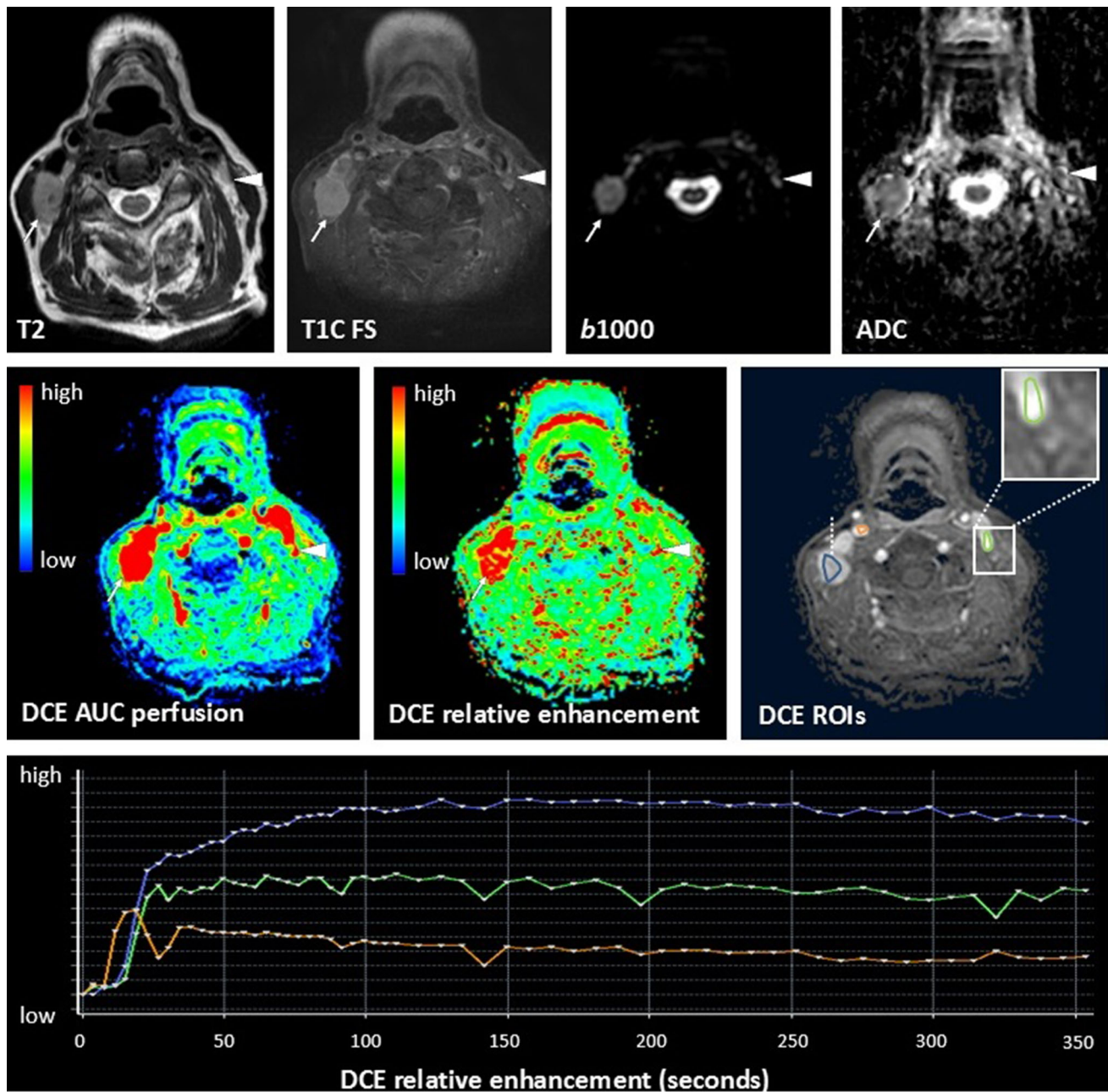
**Fig. 5** Nodal metastasis with positive diffusion and perfusion. Same patient as in Fig. 4 showing a lymph node metastasis with necrotic center with high T2 signal and no enhancement or increased perfusion (arrow head). Peripheral enhancement corresponded with high AUC (arrows) (Color figure online)

some consider the influence of perfusion below clinical relevance [65]. As the clinical implication of multiple *b* values is not yet firmly established, the acquisition of multiple *b* values in clinical setting can be questioned. However, multiple *b* values are clearly preferred in a research setting.

With respect to DCE perfusion, an increased scan duration with approximately 7–10 min is most hindering clinical applicability next to the potential artifact as discussed above [24••]. DCE perfusion is least influenced by artifacts and currently best suited to perform in patients with HNSCC. Post-processing of perfusion is more complex due to the nonspecific nature of vessel leakage resulting in possible false-negatives and false-positive results. Perfusion post-processing also has a greater range of methods and functional parameters for analysis that are available if compared to DWI [24••, 25••, 41]. This adds to the complexity of perfusion imaging and its clinical implementation.
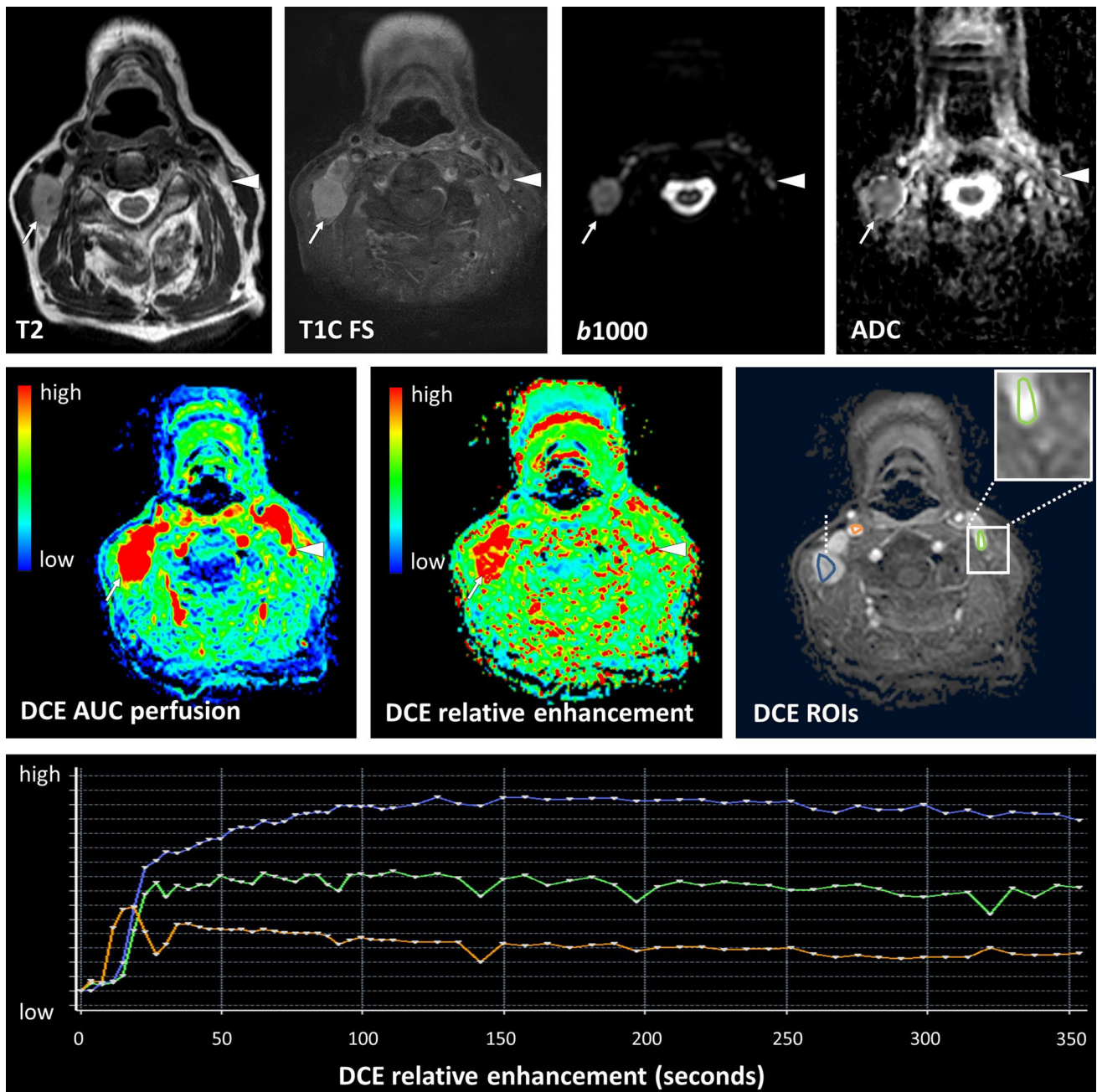
**Fig. 6** Normal lymph node and nodal metastasis with diffusion and perfusion. A 66-year-old patient with a right sided pT1N1Mx floor of the mouth SCC demonstrated recurrent lymph nodes after postoperative radiation therapy. An enlarged metastasis lymph node was seen on the right side with diffusion restriction and increased relative enhancement and AUC (arrow). A contralateral lymph node was not enlarged and demonstrated slightly restricted diffusion as is also seen in normal lymphoid tissue. Perfusion showed a high AUC and relative enhancement with a rapid wash-in with plateau phase for both lymph nodes, although most pronounced in the metastatic lymph node. Interpretation of the perfusion of lymph nodes remains difficult and should be further investigated (Color figure online)

Studies with regards to MRS suggest a higher choline-to-creatine ratio in patients with poor prognosis, which corresponds with expected high rates of proliferation and membrane biosynthesis in aggressive tumors (increased rate of metabolism) [48]. However, MRS is not commonly used due to its technical challenges. The region of interest should be placed by a radiologist to ensure correct placement in the anatomically difficult head and neck area. Furthermore, motion artifact from the carotid artery, long scan durations and complex post-processing hinders clinical applicability [52, 66].

## Future Developments and Challenges

Differentiation between malignancy and benign post-treatment effects such as fibrosis in HNSCC is of importance to guide clinical decisions. The head and neck is an area sensitive for artifacts and functional MR imaging requires advanced MRI post-processing software to evaluate HNSCC. Combined functional sequences are required to fully appreciate HNSCC post-therapy, in addition to the necessary anatomical sequences. This would result in long scan durations, but new developments could overcome time issues. A possible role of hybrid integrated PET/MR imaging might be demonstrated offering the potential to acquired anatomical and function data using different modalities. However, future research is needed to evaluate PET/MRI and its appropriate applications compared to existing techniques [67] and whether PET/MRI is of greater clinical value than PET/CT and retrospective image fusion techniques [68]. HNSCC is common and local residual and/or recurrence and nodal metastasis are seen in many patients. Diffusion is already frequently used. However, diffusion with multiple *b* values and perfusion required further confirmation of their added value in the post-therapy setting before wide-spread implementation. This is even more the case for spectroscopy. Future studies should focus on the added value of the different functional MRI sequences preferable by large prospective longitudinal multicenter studies comparing all sequences in the same population.

These studies are needed to assess the diagnostic accuracy of the functional MRI sequences separately and in combination. Another important aspect of these studies should be to define the optimum time for assessment of metabolic and physiological MRI parameters using functional techniques. The functional parameters should be tested in relation to the histopathological changes in HNSCC, treatment effects and patient outcomes. These new trials must result in standardized cut-off values and ratios for the anatomical and functional MRI sequences to precisely define post-therapy changes from tumor progression. The use of standardized cut-off values might remain arbitrary because of the use of different MRI systems. Nevertheless, it would be a valuable guideline for the clinician in daily practice. Despite these possible limitations, implications into clinical practice would be an important step in making an accurate treatment decisions for HNSCC patients.

## Conclusions

In summary, this review analyzed the role of specific functional MRI modalities in differentiating benign post-treatment effects from recurrence and/or residual malignancy and metastases in HNSCC.

Differentiation between malignant and benign post-treatment effects in HNSCC is of importance to guide clinical decisions. As anatomical MRI is not able to reliably differentiate post-therapy effect from tumor, functional techniques have been investigated and shown to be promising. This review showed that DWI can increase the diagnostic accuracy significantly for the primary tumor site and might also increase the diagnostic accuracy for the region lymph nodes after therapy. Diffusion is most easy to implement and is recommended to perform routinely in a clinical setting in HNSCC follow-up. Its use during treatment to predict outcome is interesting, but evidence is too low to implement.

Although perfusion parameters might be increased in tumor residual or recurrence and nodal metastasis, its diagnostic accuracy has yet to be established and is not routinely used clinically. DCE is least hindered by artifact and might be performed clinically if local experience is present.

Spectroscopy research is promising, but evidence is too sparse for clinical implementation in the near future. The role of hybrid PET/MR imaging is to be established.

**Compliance with Ethical Guidelines**

**Conflict of interest** Roland Nooij, Jan Hof, Peter Jan van Laar, and Anouk van der Hoorn each declare that they have no conflicts of interest.

**Human and Animal Rights and Informed Consent** This article does not contain any studies with human or animal subjects performed by the authors.

## References

Paper of particular interest, published recently, have been highlighted as:
- Of importance
- •• Of major importance

1. Fitzmaurice C, Allen C, Barber RM, Barregard L, Bhutta ZA, Brenner H, et al. Global, regional, and national cancer incidence, mortality, years of life lost, years lived with disability, and disability-adjusted life-years for 32 cancer groups, 1990 to 2015: a systematic analysis for the global burden of disease study. JAMA

Oncol. 2017;3:524–48. https://doi.org/10.1001/jamaoncol.2016.5688.

2. Gatta G, Botta L, Sánchez MJ, Anderson LA, Pierannunzio D, Licitra L. Prognoses and improvement for head and neck cancers diagnosed in Europe in early 2000s: the EUROCARE-5 population-based study. Eur J Cancer. 2015;51:2130–43. https://doi.org/10.1016/j.ejca.2015.07.043.

3. Siegel RL, Miller KD, Jemal A. Cancer statistics, 2017. CA Cancer J Clin. 2017;67:7–30. https://doi.org/10.3322/caac.21387.

4. Jou A, Hess J. Epidemiology and molecular biology of head and neck cancer. Oncol Res Treat. 2017;40:328–32. https://doi.org/10.1159/000477127.

5. Argiris A, Karamouzis MV, Raben D, Ferris RL. Head and neck cancer. Lancet. 2008;371:1695–709. https://doi.org/10.1016/S0140-6736(08)60728-X.

6. Seiwert TY, Salama JK, Vokes EE. The chemoradiation paradigm in head and neck cancer. Nat Clin Pract Oncol. 2007;4:156–71. https://doi.org/10.1038/ncponc0750.

7. Cooper JS, Pajak TF, Forastiere A, Jacobs J, Fu KK, Ang KK, et al. Precisely defining high-risk operable head and neck tumors based on RTOG#85-03 and #88-24: targets for postoperative radiochemotherapy. Head Neck. 1998;20:588–94. https://doi.org/10.1002/(SICI)1097-0347(199810)20:7<588:AID-HED2>3.0.CO;2-F.

8. Jacob LA, Chaudhuri T, Lakshmaiah KC, Babu KG, Dasappa L, Babu MCS, et al. Current status of systemic therapy for recurrent and/or metastatic squamous cell carcinoma of the head and neck. Indian J Cancer. 2016;53:471–7. https://doi.org/10.4103/0019-509X.204786.

9. Overgaard J, Hansen HS, Specht L, Overgaard M, Grau C, Andersen E, et al. Five compared with six fractions per week of conventional radiotherapy of squamous-cell carcinoma of head and neck: DAHANCA 6 and 7 randomised controlled trial. Lancet. 2003;362:933–40. https://doi.org/10.1016/S0140-6736(03)14361-9.

10. •• Saito N, Nadgir RN, Nakahira M, Takahashi M, Uchino A, Kimura F, et al. Posttreatment CT and MR imaging in head and neck cancer: What the radiologist needs to know. Radiographics 2012;32:1261–82. https://doi.org/10.1148/rg.325115160. *Normal postoperative imaging findings and complications in patients with HNSCC on CT and anatomical MRI are demonstrated. Some examples of the applicability of DWI are also discussed from a radiologist perspective.*

11. Maroldi R, Ravanelli M, Farina D. Magnetic resonance for laryngeal cancer. Curr Opin Otolaryngol Head Neck Surg. 2014;22:131–9. https://doi.org/10.1097/MOO.0000000000000036.

12. Bhatnagar P, Subesinghe M, Patel C, Prestwich R, Scarsbrook AF. Functional imaging for radiation treatment planning, response assessment, and adaptive therapy in head and neck cancer. Radiographics. 2013;33:1909–29. https://doi.org/10.1148/rg.337125163.

13. • Al-Shwaiheen FA, Wang SJ, Uzelac A, Yom SS, Ryan WR. The advantages and drawbacks of routine magnetic resonance imaging for long-term posttreatment locoregional surveillance of oral cavity squamous cell carcinoma. Am J Otolaryngol 2015;36:415–23. https://doi.org/10.1016/j.amjoto.2015.01.024. *Analysis of routinely performed MRI with regards to treated squamous cell carcinoma of the oral cavity. Advantages and drawbacks with regards to false positives and false negatives on MRI in patients without suspicious clinical or exam findings are discussed.*

14. • Gage KL, Thomas K, Jeong D, Stallworth DG, Arrington JA. Multimodal imaging of head and neck squamous cell carcinoma. Cancer Control 2017;24:172–9. *Evaluation of advanced HNSCC for treatment planning and follow up through multimodal imaging. PET/CT and anatomical MRI are discussed. Functional MRI is not discussed.*

15. Omura G, Saito Y, Ando M, Kobayashi K, Ebihara Y, Yamasoba T, et al. Salvage surgery for local residual or recurrent pharyngeal cancer after radiotherapy or chemoradiotherapy. Laryngoscope. 2014;124:2075–80. https://doi.org/10.1002/lary.24695.

16. Camisasca DR, Silami MANC, Honorato J, Dias FL, de Faria PAS, Lourenço SdQC. Oral squamous cell carcinoma: clinicopathological features in patients with and without recurrence. ORL J Otorhinolaryngol Relat Spec. 2011;73:170–6. https://doi.org/10.1159/000328340.

17. Guo T, Qualliotine JR, Ha PK, Califano JA, Kim Y, Saunders JR, et al. Surgical salvage improves overall survival for patients with HPV-positive and HPV-negative recurrent locoregional and distant metastatic oropharyngeal cancer. Cancer. 2015;121:1977–84. https://doi.org/10.1002/cncr.29323.

18. Kim S-A, Roh J-L, Kim JS, Lee JH, Lee SH, Choi S-H, et al. (18)F-FDG PET/CT surveillance for the detection of recurrence in patients with head and neck cancer. Eur J Cancer. 2017;72:62–70. https://doi.org/10.1016/j.ejca.2016.11.009.

19. Castaldi P, Leccisotti L, Bussu F, Miccichè F, Rufini V. Role of 18F-FDG PET-CT in head and neck squamous cell carcinoma. Acta Otorhinolaryngol Ital. 2013;33:1–8.

20. Helsen N, Roothans D, van den Heuvel B, van den Wyngaert T, van den Weyngaert D, Carp L, et al. 18F-FDG-PET/CT for the detection of disease in patients with head and neck cancer treated with radiotherapy. PLoS ONE. 2017;12:e0182350. https://doi.org/10.1371/journal.pone.0182350.

21. Mak D, Corry J, Lau E, Rischin D, Hicks RJ. Role of FDG-PET/CT in staging and follow-up of head and neck squamous cell carcinoma. Q J Nucl Med Mol Imaging. 2011;55:487–99.

22. •• van der Hoorn A, van Laar PJ, Holtman GA, Westerlaan HE. Diagnostic accuracy of magnetic resonance imaging techniques for treatment response evaluation in patients with head and neck tumors, a systematic review and meta-analysis. PLoS One 2017;12:e0177986. https://doi.org/10.1371/journal.pone.0177986. *A meta-analysis summarizing all available diagnostic accuracy of DWI studies for the treatment evaluation of SCC head and neck tumors for the primary tumor site and lymph nodes.*

23. de Bondt RBJ, Nelemans PJ, Bakers F, Casselman JW, Peutz-Kootstra C, Kremer B, et al. Morphological MRI criteria improve the detection of lymph node metastases in head and neck squamous cell carcinoma: multivariate logistic regression analysis of MRI features of cervical lymph nodes. Eur Radiol. 2009;19:626–33. https://doi.org/10.1007/s00330-008-1187-3.

24. •• Jansen JFA, Parra C, Lu Y, Shukla-Dave A. Evaluation of head and neck tumors with functional MR imaging. Magn Reson Imaging Clin N Am 2016;24:123-33. https://doi.org/10.1016/j.mric.2015.08.011. *This review describes the use of functional MRI sequences in head and neck cancer including detailed description of protocols.*

25. •• King AD, Thoeny HC. Functional MRI for the prediction of treatment response in head and neck squamous cell carcinoma: potential and limitations. Cancer Imaging 2016;16:23. https://doi.org/10.1186/s40644-016-0080-6. *Review of role and potential of functional MRI during and after treatment, focussing on DWI (also grants insight in % rise ADC early in treatment in unfavourable treatment outcome) and Ktrans from DCE-MRI. Also discusses possibility of MRS.*

26. King AD, Chow K-K, Yu K-H, Mo FKF, Yeung DKW, Yuan J, et al. Head and neck squamous cell carcinoma: diagnostic performance of diffusion-weighted MR imaging for the prediction of treatment response. Radiology. 2013;266:531–8. https://doi.org/10.1148/radiol.12120167.

27. Marzi S, Piludu F, Sanguineti G, Marucci L, Farneti A, Terrenato I, et al. The prediction of the treatment response of cervical nodes using intravoxel incoherent motion diffusion-weighted imaging. Eur J Radiol. 2017;92:93–102. https://doi.org/10.1016/j.ejrad.2017.05.002.

28. Liang L, Luo X, Lian Z, Chen W, Zhang B, Dong Y, et al. Lymph node metastasis in head and neck squamous carcinoma: efficacy of intravoxel incoherent motion magnetic resonance imaging for the differential diagnosis. Eur J Radiol. 2017;90:159–65. https://doi.org/10.1016/j.ejrad.2017.02.039.

29. • Paudyal R, Oh JH, Riaz N, Venigalla P, Li J, Hatzoglou V, et al. Intravoxel incoherent motion diffusion-weighted MRI during chemoradiation therapy to characterize and monitor treatment response in human papillomavirus head and neck squamous cell carcinoma. J Magn Reson Imaging 2017;45:1013–23. https://doi.org/10.1002/jmri.255. *This study showed the utility of IVIM DWI for early assessment of treatment response of chemoradiation therapy in HNSCC patients. D and f values as indicators are also discussed.*

30. Sasaki M, Sumi M, Eida S, Katayama I, Hotokezaka Y, Nakamura T. Simple and reliable determination of intravoxel incoherent motion parameters for the differential diagnosis of head and neck tumors. PLoS ONE. 2014;9:e112866. https://doi.org/10.1371/journal.pone.0112866.

31. Zheng D, Chen Y, Liu X, Chen Y, Xu L, Ren W, et al. Early response to chemoradiotherapy for nasopharyngeal carcinoma treatment: value of dynamic contrast-enhanced 3.0 T MRI. J Magn Reson Imaging. 2015;41:1528–40. https://doi.org/10.1002/jmri.24723.

32. Sumi M, Nakamura T. Head and neck tumors: assessment of perfusion-related parameters and diffusion coefficients based on the intravoxel incoherent motion model. AJNR Am J Neuroradiol. 2013;34:410–6. https://doi.org/10.3174/ajnr.A3227.

33. • Abdel Razek AAK, Gaballa G, Ashamalla G, Alashry MS, Nada N. Dynamic susceptibility contrast perfusion-weighted magnetic resonance imaging and diffusion-weighted magnetic resonance imaging in differentiating recurrent head and neck cancer from postradiation changes. J Comput Assist Tomogr 2015;39:849–54. https://doi.org/10.1097/rct.0000000000000311. *This study shows the possibilities of ADC-values and DSC perfusion-weighted MR imaging, in the differentiation of recurrent head and neck cancer from postradiation changes.*

34. Verduijn GM, Bartels LW, Raaijmakers CPJ, Terhaard CHJ, Pameijer FA, van den Berg CAT. Magnetic resonance imaging protocol optimization for delineation of gross tumor volume in hypopharyngeal and laryngeal tumors. Int J Radiat Oncol Biol Phys. 2009;74:630–6. https://doi.org/10.1016/j.ijrobp.2009.01.014.

35. Bertrand M, Tollard E, Francois A, Bouchetemble P, Marie PJ, Dehesdin D, et al. CT scan, MR imaging and anatomopathologic correlation in the glottic carcinoma T1-T2. Rev Laryngol Otol Rhinol (Bord). 2010;131:51–7.

36. Ravanelli M, Farina D, Rizzardi P, Botturi E, Prandolini P, Mangili S, et al. MR with surface coils in the follow-up after endoscopic laser resection for glottic squamous cell carcinoma: feasibility and diagnostic accuracy. Neuroradiology. 2013;55:225–32. https://doi.org/10.1007/s00234-012-1128-3.

37. Zbaren P, Becker M, Lang H. Pretherapeutic staging of laryngeal carcinoma. Clinical findings, computed tomography, and magnetic resonance imaging compared with histopathology. Cancer. 1996;77:1263–73. https://doi.org/10.1001/archotol.1997.01900090016003.

38. Chikui T, Kitamoto E, Kawano S, Sugiura T, Obara M, Simonetti AW, et al. Pharmacokinetic analysis based on dynamic contrast-enhanced MRI for evaluating tumor response to preoperative therapy for oral cancer. J Magn Reson Imaging. 2012;36:589–97. https://doi.org/10.1002/jmri.23704.

39. Cao Y, Popovtzer A, Li D, Chepeha DB, Moyer JS, Prince ME, et al. Early prediction of outcome in advanced head-and-neck cancer based on tumor blood volume alterations during therapy: a prospective study. Int J Radiat Oncol Biol Phys. 2008;72:1287–90. https://doi.org/10.1016/j.ijrobp.2008.08.024.

40. Ng S-H, Lin C-Y, Chan S-C, Yen T-C, Liao C-T, Chang JT-C, et al. Dynamic contrast-enhanced MR imaging predicts local control in oropharyngeal or hypopharyngeal squamous cell carcinoma treated with chemoradiotherapy. PLoS ONE. 2013;8:e72230. https://doi.org/10.1371/journal.pone.0072230.

41. Fujima N, Kudo K, Yoshida D, Homma A, Sakashita T, Tsukahara A, et al. Arterial spin labeling to determine tumor viability in head and neck cancer before and after treatment. J Magn Reson Imaging. 2014;40:920–8. https://doi.org/10.1002/jmri.24421.

42. Fujima N, Kudo K, Tsukahara A, Yoshida D, Sakashita T, Hommaet A, et al. Measurement of tumor blood flow in head and neck squamous cell carcinoma by pseudo-continuous arterial spin labeling: comparison with dynamic contrast-enhanced MRI. J Magn Reson Imaging. 2015;41:983–91. https://doi.org/10.1002/jmri.24885.

43. Devpura S, Barton KN, Brown SL, Palyvoda O, Kalkanis S, Naik VM, et al. Vision 20/20: the role of Raman spectroscopy in early stage cancer detection and feasibility for application in radiation therapy response assessment. Med Phys. 2014;41:050901. https://doi.org/10.1118/1.4870981.

44. Hwang I, Choi SH, Kim Y-J, Kim KG, Lee AL, Yun TJ, et al. Differentiation of recurrent tumor and posttreatment changes in head and neck squamous cell carcinoma: application of high b-value diffusion-weighted imaging. AJNR Am J Neuroradiol. 2013;34:2343–8. https://doi.org/10.3174/ajnr.A3603.

45. Vandecaveye V, Dirix P, de Keyzer F, de Beeck K, vander Poorten V, Roebben I, et al. Predictive value of diffusion-weighted magnetic resonance imaging during chemoradiotherapy for head and neck squamous cell carcinoma. Eur Radiol. 2010;20:1703–14. https://doi.org/10.1007/s00330-010-1734-6.

46. Matoba M, Tuji H, Shimode Y, Toyoda I, Kuginuki Y, Miwa K, et al. Fractional change in apparent diffusion coefficient as an imaging biomarker for predicting treatment response in head and neck cancer treated with chemoradiotherapy. AJNR Am J Neuroradiol. 2014;35:379–85. https://doi.org/10.3174/ajnr.A3706.

47. Bernstein JM, Kershaw LE, Withey SB, Lowe NM, Homer JJ, Slevin NJ, et al. Tumor plasma flow determined by dynamic contrast-enhanced MRI predicts response to induction chemotherapy in head and neck cancer. Oral Oncol. 2015;51:508–13. https://doi.org/10.1016/j.oraloncology.2015.01.013.

48. Bezabeh T, Odlum O, Nason R, Kerr P, Sutherland D, Patel R, et al. Prediction of treatment response in head and neck cancer by magnetic resonance spectroscopy. AJNR Am J Neuroradiol. 2005;26:2108–13.

49. Acampora A, Manzo G, Fenza G, Busto G, Serino A, Manto A. High b-Value Diffusion MRI to differentiate recurrent tumors from posttreatment changes in head and neck squamous cell carcinoma: a single center prospective study. Biomed Res Int. 2016;2016:2865169. https://doi.org/10.1155/2016/2865169.

50. Choi SH, Lee JH, Choi YJ, Park JE, Sung YS, Kim N, et al. Detection of local tumor recurrence after definitive treatment of head and neck squamous cell carcinoma: histogram analysis of dynamic contrast-enhanced T1-weighted perfusion MRI. AJR Am J Roentgenol. 2017;208:42–7. https://doi.org/10.2214/AJR.16.16127.

51. Choi YJ, Lee JH, Sung YS, Yoon RG, Park JE, Nam SY, et al. Value of dynamic contrast-enhanced MRI to detect local tumor

recurrence in primary head and neck cancer patients. Medicine. 2016;95:e3698. https://doi.org/10.1097/MD.0000000000003698.

52. King AD, Yeung DKW, Yu K-H, Mo FKF, Hu C-W, Bhatia KS, et al. Monitoring of treatment response after chemoradiotherapy for head and neck cancer using in vivo 1H MR spectroscopy. Eur Radiol. 2010;20:165–72. https://doi.org/10.1007/s00330-009-1531-2.

53. Berrak S, Chawla S, Kim S, Quon H, Sherman E, Loevner LA, et al. Diffusion weighted imaging in predicting progression free survival in patients with squamous cell carcinomas of the head and neck treated with induction chemotherapy. Acad Radiol. 2011;18:1225–32. https://doi.org/10.1016/j.acra.2011.06.009.

54. Jin GQ, Yang J, Liu LD, Su DK, Wang DP, Zhao SF, et al. The diagnostic value of 1.5-T diffusion-weighted MR imaging in detecting 5 to 10 mm metastatic cervical lymph nodes of nasopharyngeal carcinoma. Medicine (Baltimore). 2016;95: e4286. https://doi.org/10.1097/MD.0000000000004286.

55. Holzapfel K, Duetsch S, Fauser C, Eiber M, Rummeny EJ, Gaa J. Value of diffusion-weighted MR imaging in the differentiation between benign and malignant cervical lymph nodes. Eur J Radiol. 2009;72:381–7. https://doi.org/10.1016/j.ejrad.2008.09.034.

56. Abdel Razek AAK, Soliman NY, Elkhamary S, Alsharaway MK, Tawfik A. Role of diffusion-weighted MR imaging in cervical lymphadenopathy. Eur Radiol. 2006;16:1468–77. https://doi.org/10.1007/s00330-005-0133-x.

57. Tyagi N, Riaz N, Hunt M, Wengler K, Hatzoglou V, Young R, et al. Weekly response assessment of involved lymph nodes to radiotherapy using diffusion-weighted MRI in oropharynx squamous cell carcinoma. Med Phys. 2016;43:137. https://doi.org/10.1118/1.4937791.

58. Hauser T, Essig M, Jensen A, Laun FB, Münter M, Maier-Hein KH, et al. Prediction of treatment response in head and neck carcinomas using IVIM-DWI: evaluation of lymph node metastasis. Eur J Radiol. 2014;83:783–7. https://doi.org/10.1016/j.ejrad.2014.02.013.

59. Jansen JFA, Carlson DL, Lu Y, Stambuk HE, Moreira AL, Singh B, et al. Correlation of a priori DCE-MRI and (1)H-MRS data with molecular markers in neck nodal metastases: initial analysis. Oral Oncol. 2012;48:717–22. https://doi.org/10.1016/j.oraloncology.2012.02.001.

60. King AD, Yeung DKW, Ahuja AT, Leung SF, Tse GMK, van Hasselt AC. In vivo proton MR spectroscopy of primary and nodal nasopharyngeal carcinoma. AJNR Am J Neuroradiol. 2004;25:484–90.

61. Shah GV, Gandhi D, Mukherji SK. Magnetic resonance spectroscopy of head and neck neoplasms. Top Magn Reson Imaging. 2004;15:87–94.

62. Chawla S, Kim S, Loevner LA, Quon H, Wang S, Mutale F, et al. Proton and phosphorous MR spectroscopy in squamous cell carcinomas of the head and neck. Acad Radiol. 2009;16:1366–72. https://doi.org/10.1016/j.acra.2009.06.001.

63. Hoang JK, Choudhury KR, Chang J, Craciunescu OI, Yoo DS, Brizel DM. Diffusion-weighted imaging for head and neck squamous cell carcinoma: quantifying repeatability to understand early treatment-induced change. AJR Am J Roentgenol. 2014;203:1104–8. https://doi.org/10.2214/AJR.14.12838.

64. Vaid S, Chandorkar A, Atre A, Shah D, Vaid N. Differentiating recurrent tumours from posttreatment changes in head and neck cancers: does diffusion-weighted MRI solve the eternal dilemma? Clin Radiol. 2017;72:74–83. https://doi.org/10.1016/j.crad.2016.09.019.

65. Vidiri A, Minosse S, Piludu F, Curione D, Pichi B, Spriano G, et al. Feasibility study of reduced field of view diffusion-weighted magnetic resonance imaging in head and neck tumors. Acta Radiol. 2017;58:292–300. https://doi.org/10.1177/0284185116652014.

66. Abdel Razek AAK, Poptani H. MR spectroscopy of head and neck cancer. Eur J Radiol. 2013;82:982–9. https://doi.org/10.1016/j.ejrad.2013.01.025.

67. Torigian DA, Zaidi H, Kwee TC, Saboury B, Udupa JK, Cho ZH, et al. PET/MR imaging: technical aspects and potential clinical applications. Radiology. 2013;267:26–44. https://doi.org/10.1148/radiol.13121038.

68. Loeffelbein DJ, Souvatzoglou M, Wankerl V, Martinez-Möller A, Dinges J, Schwaiger M, et al. PET-MRI fusion in head-and-neck oncology: current status and implications for hybrid PET/MRI. J Oral Maxillofac Surg. 2012;70:473–83. https://doi.org/10.1016/j.joms.2011.02.120.